Synthesis of oleanolic acid derivatives: In vitro, in vivo and in silico studies for PTP-1B inhibition

9 **AUTHORS**, INCLUDING:

Yolanda Rios Gomez
Universidad Autónoma del Estado de Morelos
86 PUBLICATIONS **662** CITATIONS

SEE PROFILE

Paolo Paoli
University of Florence
39 PUBLICATIONS **533** CITATIONS

SEE PROFILE

Gabriel Navarrete-Vázquez
Universidad Autónoma del Estado de Morelos
71 PUBLICATIONS **1,103** CITATIONS

SEE PROFILE

Samuel Estrada-Soto
Universidad Autónoma del Estado de Morelos
88 PUBLICATIONS **821** CITATIONS

SEE PROFILE

Original article

Synthesis of oleanolic acid derivatives: *In vitro*, *in vivo* and *in silico* studies for PTP-1B inhibition[☆]

Juan José Ramírez-Espinosa [a], Maria Yolanda Rios [b], Paolo Paoli [c], Virginia Flores-Morales [d], Guido Camici [c], Vianey de la Rosa-Lugo [b], Sergio Hidalgo-Figueroa [a], Gabriel Navarrete-Vázquez [a], Samuel Estrada-Soto [a, *]

[a] *Facultad de Farmacia, Universidad Autónoma del estado de Morelos, Cuernavaca, Morelos 62209, Mexico*
[b] *Centro de Investigaciones Químicas, Universidad Autónoma del Estado de Morelos, Cuernavaca, Morelos 62209, Mexico*
[c] *Dipartimento di Scienze Biomediche Sperimentali e Cliniche, Sezione di Scienze Biochimiche, Universitá degli Studi di Firenze, Viale Morgagni 50, 50134 Firenze, Italy*
[d] *Unidad Académica de Ciencias Químicas, Universidad Autónoma de Zacatecas, Zacatecas, Zacatecas 98160, Mexico*

A R T I C L E   I N F O

A B S T R A C T

Non-insulin dependent diabetes mellitus is a multifactorial disease that links different metabolic routes; a point of convergence is the enzyme PTP-1B which turns off insulin and leptin receptors involved in glucose and lipid metabolism, respectively. Pentacyclic acid triterpenes such as oleanolic acid (OA) have proved to be excellent PTP-1B inhibitors, thus, the purpose of current work was to generate a series of derivatives that improve the pharmacological effect of OA. Our findings suggest that the presence of the carboxylic acid and/or its corresponding reduction product carbinol derivative (H-bond donor) in C-28 is required to maintain the inhibitory activity; moreover, this is further enhanced by ester or ether formation on C-3. The most active derivatives were cinnamoyl ester (**6**) and ethyl ether (**10**). Compound **6** showed potent *in vitro* inhibitory activity and significantly decrease of blood glucose levels on *in vivo* experiments. Meanwhile, **10** showed contrasting outcomes, since it was the compound with higher inhibitory activity and selectivity over PTP-1B and has improved interaction with site B, according with docking studies, the *in vivo* antidiabetic effect was similar to oleanolic acid. In conclusion, oleanolic acid derivatives have revealed an enhanced inhibitory effect over PTP-1B activity by increasing molecular interactions with either catalytic or allosteric sites and producing a hypoglycaemic effect on non insulin dependent diabetes mellitus rat model.

© 2014 Elsevier Masson SAS. All rights reserved.

1. Introduction

The phosphorylation of protein tyrosyl residues is an important regulation point over several signalling pathways implicated in cell metabolism, proliferation and differentiation. Insulin begins its biological action by binding to the insulin receptor (IR), which is a tyrosine kinase, causing autophosphorylation of tyrosine residues and posterior activation of IR substrates and downstream signal propagation. Also, the binding of leptin to its receptor leads a phosphorylation of Janus kinase 2 (JAK-2) activating the JAK signal transduction [1]. The protein tyrosine phosphatase 1B is an enzyme that negatively regulates IR and leptin pathways by catalysing the dephosphorylation of cellular substrates. Thus, PTP-1B inhibition represents a therapeutic target to develop new drugs for the treatment of diabetes and obesity, causing that IR and leptin receptors longer be active for their agonist. So, several compounds have been proposed for non-insulin dependent diabetes mellitus (NIDDM) treatment using medicinal chemistry tools, especially structure-based drug design. Unfortunately, the endeavour to develop therapeutic drugs from synthetic and natural PTP-1B inhibitors bioactive molecules has not advanced [2].

On the other hand, natural products with triterpenic acid scaffolds have shown hypoglycaemic effect mediated by PTP-1B inhibition over few *in vitro* and *in vivo* diabetic and obese models. In this sense, oleananes have a gem-dimethyl group at C-20 and stands as promising natural products for glucose control through several mechanisms, especially those related with enzymatic inhibition and cellular signalling. Oleanolic acid has shown an improvement regulation of glucose levels over diverse *in vivo*
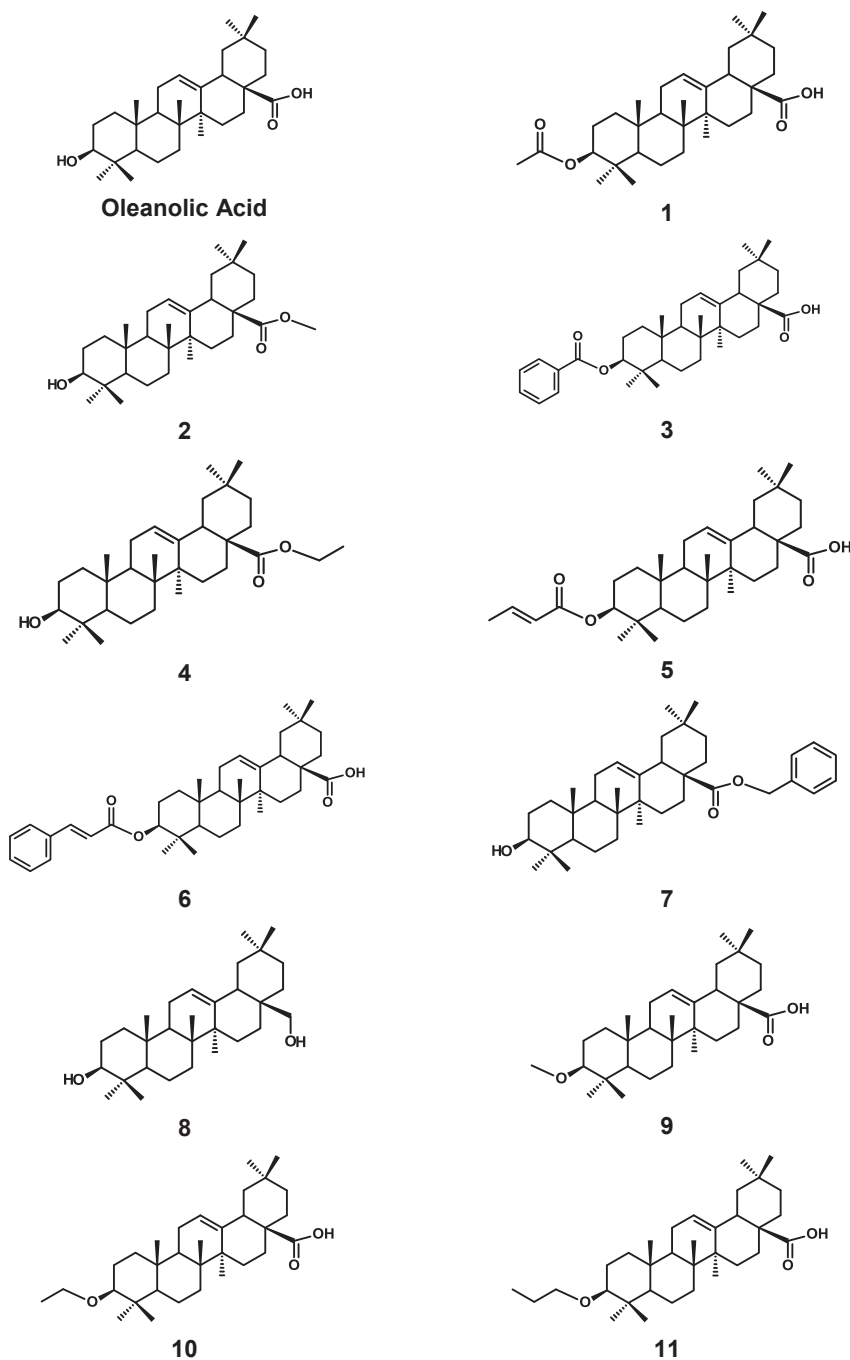
Fig. 1. Chemical structure of oleanolic acid derivatives.

diabetic models, proposing that enhancement of hepatic glycogen synthesis, leptin/ghrelin modulation, insulin sensitivity and diminution of serum glucose, cholesterol, triglycerides and LDL are the primordial effects; based on molecular and *in vitro* studies, protein tyrosine phosphatase 1B (PTP-1B) inhibition seems to be the main mechanism of action, but others as PPARs agonist, AKT stimulation, AMPK activation or inclusive insulin secretion have been described [3]. In this context, oleanolic acid has been proposed as a lead for guided drug design with hypoglycaemic effect by improving its inhibitory activity over several known targets, particularly PTP-1B enzyme. Among them, there are several derivatives by changing C-3 hydroxy, C-12 double bond or C-28 carboxylic acid for aryl or

alkyl substituents in order to improve their inhibitory activity, also glycosides derivatives in the same positions have increased both solubility and PTP-1B inhibition [4].

As a final point, oleanolic acid is a promising drug for diabetes treatment, its selectivity for PTP-1B and *in vivo* hypoglycaemic effect make it a hit molecule for more potent and selective drugs. Looking for better pharmacological properties, in current work we synthesize a series of oleanolic acid derivatives and report their *in vitro* and *in silico* inhibition of PTP-1B, as well as the *in vivo* effect of those more active.

2. Results and discussion
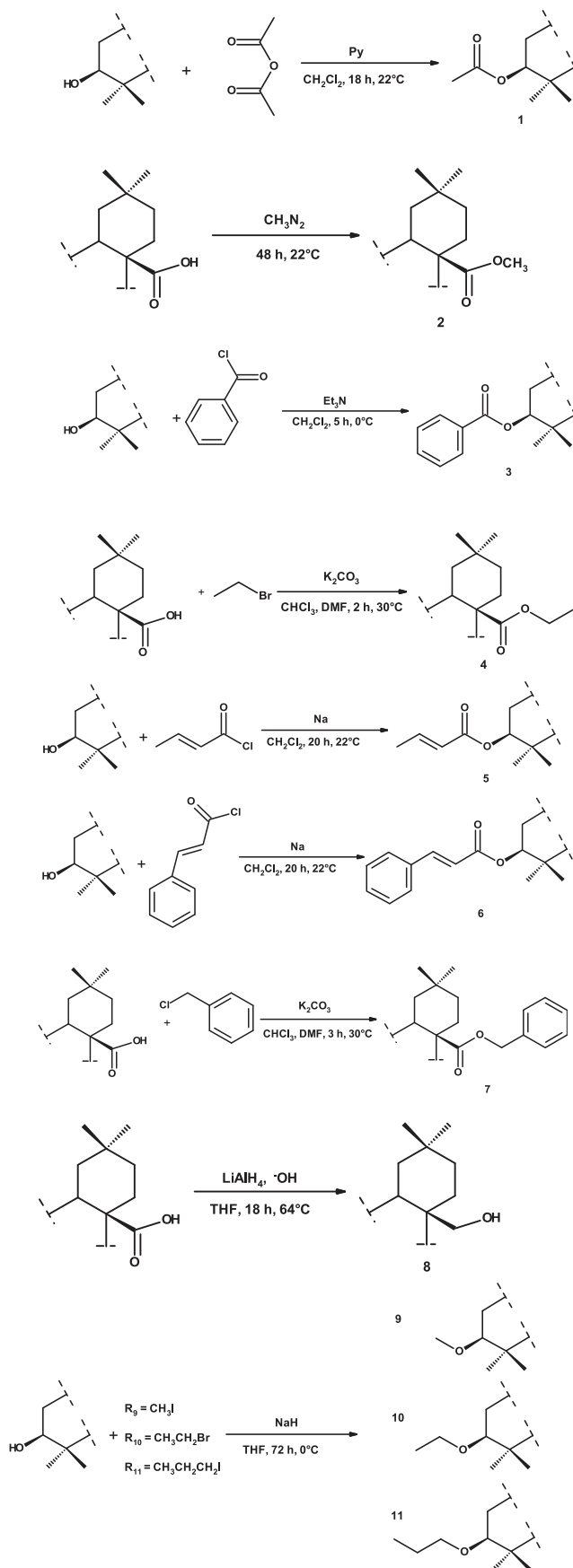
2.1. Synthesis of oleanolic acid derivatives

The design of PTP-1B inhibitors is based on four approaches: 1) identification of pro-drugs that improve bioavailability of compounds, 2) design of drugs with capability of interact with both catalytic and allosteric sites of PTP-1B enzyme, 3) discovery of inhibitors that could be orally administered with reduced side effects and 4) evaluation of the degree which inhibitor prevents or treats NIDDM or obesity and their complications [5]. Following these suggestions, eleven derivatives of oleanolic acid were prepared (Fig. 1): four esters and three ethers on C-3 hydroxyl, three esters from C-28 carboxylic acid and the corresponding primary alcohol derived from reduction of carboxylic acid with LiAlH$_4$. All esters were prepared by classical methods using acyl chlorides, alkyl halides or anhydrides in presence of an appropriate base as indicated. Acetylation of oleanolic acid with acetic anhydride using pyridine as catalyst allows 3-acetyl-oleanolic acid synthesis with 38% yield which was independent from pyridine excess. Microwave assisted methods were determinant to obtain 3-crotonyl-oleanolic acid, 3-cinnamoyl-oleanolic acid or C-3 ethyl and benzyl esters, which allows an improvement performance of reaction times. Homologated ethers were prepared with Me, Et and *n*-Pr halides and metallic sodium improved the reaction performance, suggesting that metallic sodium is the best base for this reactions (Scheme 1).

### 2.2. In vitro PTP-1B screening

To screen the inhibitory properties of oleanolic acid derivatives against PTP-1B, we carried out initial assays using both single substrate and single inhibitor concentration. The mixture containing an aliquot of enzyme was incubated with a fixed substrate concentration (3 mM) and 50 μM of the test samples (final concentration). The control experiment was carried out adding DMSO in the sample assay. Results are reported in Fig. 2, showing that **1**, **3**, **5**, **6**, **8**, **9**, **10** and **11** strongly inhibit PTP-1B; in fact, the presence of 50 μM of each compound inhibits 85—99% of enzyme respect to the control test. In contrast, **2**, **4** as well as **7** behave as weak inhibitors, confirming that the presence of the carboxylic acid and/or its corresponding reduction product carbinol derivative (H-bond donor) in C-28 is required to maintain the inhibitory activity. For better evaluation of the inhibitory activity of all active compounds, their IC$_{50}$ values were measured (Table 1 and Fig. 3). For each compound, the enzymatic activity of PTP-1B was determined in the presence of increasing inhibitor concentrations; the normalized residual activity values were reported in graphic versus inhibitor concentration and fitted by using Eq. (1) to calculate IC$_{50}$ values. In Eq. (1), V_i/V_0 is the ratio between the measured activity in the presence of the inhibitor (V_i) and the activity of the control without the inhibitor (V_0), and "x" is the inhibitor concentration, Max and Min, the maximal and minimal enzymatic activity observed, respectively. From that, it was established that **6** and **10** were the most active compounds even than oleanolic acid [6], fact that justified current investigation.

$$V_i \Big/ V_0 = \frac{\mathrm{Max} - \mathrm{Min}}{\left(1 + \frac{x}{\mathrm{IC}_{50}}\right)^p} + \mathrm{Min} \qquad (1)$$

In order to determine the type of inhibition, we analysed experimental data by the double reciprocal plot method. For each compound, we measured the initial hydrolysis rate using seven substrate final concentrations (0.5—25 mM range), in the presence of increasing concentrations of each compound. Compounds **6** and

Scheme 1. Reagents and conditions for the synthesis of oleanolic acid derivatives.
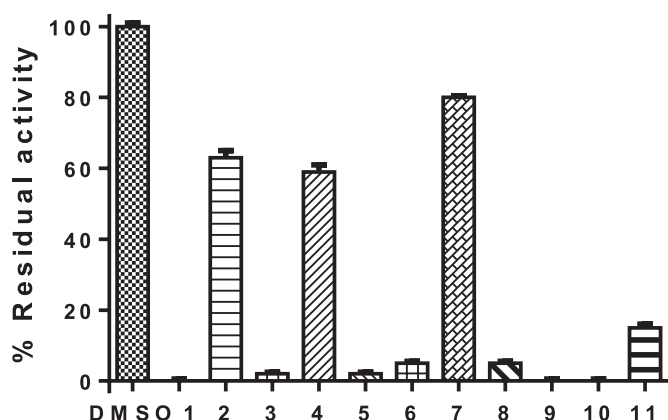
Fig. 2. Preliminary screening with PTP-1B. All assays were carried out at the final inhibitor concentration of 50 μM. The assay solution was prepared dissolving the substrate (*p*-nitrophenylphosphate, 3 mM final concentration) in β,β-dimethylgluta-rate buffer pH 7.0, containing 1 mM EDTA and 1 mM dithiothreitol. The final volume was 1 ml; all assays were carried out at 37 °C. Each assay was performed in triplicate. The values reported represent the mean value ± S.E.M.

Table 1
Assay for reversibility of inhibition and IC_{50} values determined for different PTPases. Aliquots of PTP-1B were incubated in the presence of 10-times IC_{50} concentration of each compound for 1 h (white bars) or 2 h (black bars) at 37 °C. After incubation, the enzyme was diluted 250-fold with the assay solution (37 °C, 25 mM pNPP) to measure the residual activity. Control experiments was carried out adding DMSO. For each inhibitor, 15–18 concentrations of inhibitor were used. The data reported in the table represent the value ± S.E.M. of triplicates.

Compound	% Of reversibility	IC_{50} (μM)			
		PTP1B	TC-PTP	IF1	IF2
Oleanolic acid	70	9.5 ± 0.5	–	21.2 ± 0.5	22.9 ± 0.9
1	75	21.5 ± 2.5	No determined		
3	77	16.2 ± 0.4			
5	80	17.8 ± 0.4			
6	95	6.1 ± 0.3	11.8 ± 0.5	6.9 ± 0.3	12.3 ± 0.4
8	70	9.6 ± 0.2	No determined		
9	80	8.6 ± 0.4			
10	95	5.3 ± 0.2	26.0 ± 2.8	16.4 ± 1	47.4 ± 3
11	67	36.5 ± 1.6	No determined		

10, which are the most active PTP1B inhibitors, were selected for kinetic studies. They produced two different plot types as follows: compound **6** behaved as mixed-type inhibitor, since its graph showed straight lines that intersect each other at the left panel (Fig. 4, top panel). Later was confirmed by the fact that increasing inhibitor concentration is accompanied by increase of Km values and decrease of V_{max} values (Fig. 4, middle and bottom panels, respectively). The mixed-type inhibitor model, shown in Scheme 2B, indicates that the inhibitor binds both E and ES. In this case, EI has lower affinity for S than E ($\alpha > 1$), and ESI is non-productive.

On the other hand, **10** acted as non-competitive inhibitor, since the graph showed straight lines that intersect each other on the abscissa axis (Fig. 5, top panel). It was confirmed by the fact that increasing inhibitor concentration, the Km values remained almost constant while Vmax values decreased (Fig. 5, middle panel and bottom panel, respectively). In the non-competitive model, shown in Scheme 2A, the inhibitor is capable to bind both E and the enzyme—substrate complex (ES), and the enzyme-substrate-inhibitor ternary complex (ESI) is non-productive. For each compound we calculated the K_i value, using the appropriate equations. Results obtained in this experiment are reported in Table 2. The above inhibition types are in agreed with the docking results shown at the bottom.

The selectivity of compounds **6** and **10** were evaluated by determining the IC_{50} values for three additional PTPs, such as human TC-PTP, which is structurally correlated with PTP-1B, and isoenzymes IF1 and IF2 of human LMW-PTP. Results are summarized in Table 1, which indicate that **10** is more selective for PTP-1B than other related protein phosphatases, however **6** did not showed that selectivity. Nonetheless, both of them have potential to be developed as new antidiabetic drugs. Further experiments are necessary to probe that asseveration.

Finally, reversibility assays were performed for determining the capability of PTP-1B to restore its enzymatic activity after treatment with the most active compounds during one or 2 h. Reversibility of oleanolic acid was described previously, inhibiting 30% of enzyme activity in a permanently manner, which is the case for all derivatives (Table 1), except for **6** and **10** who permanently inhibited the enzymatic activity only by 5%.

2.3. In vivo hypoglycaemic effect

The hypoglycaemic effect of the most active PTP-1B inhibitors, compounds **6** and **10**, were evaluated on NIDDM rat model. 50 mg/kg of both derivatives induced a sustained decrease of blood
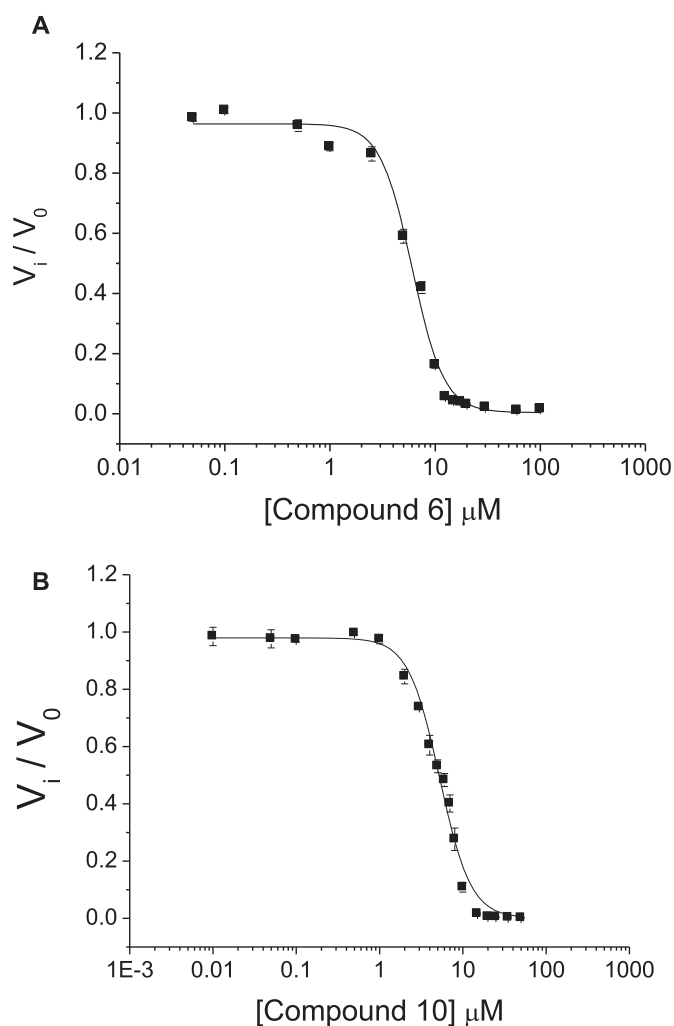
Fig. 3. IC_{50} determination. The IC_{50} were determined by plotting the residual activity versus inhibitor concentration. Only compounds **6** (A) and **10** (B) are shown. 15-18 different concentrations were used for each inhibitor. All assays were performed in quadruplicate. Data represent the mean ± S.E.M.

A)

B)

C)
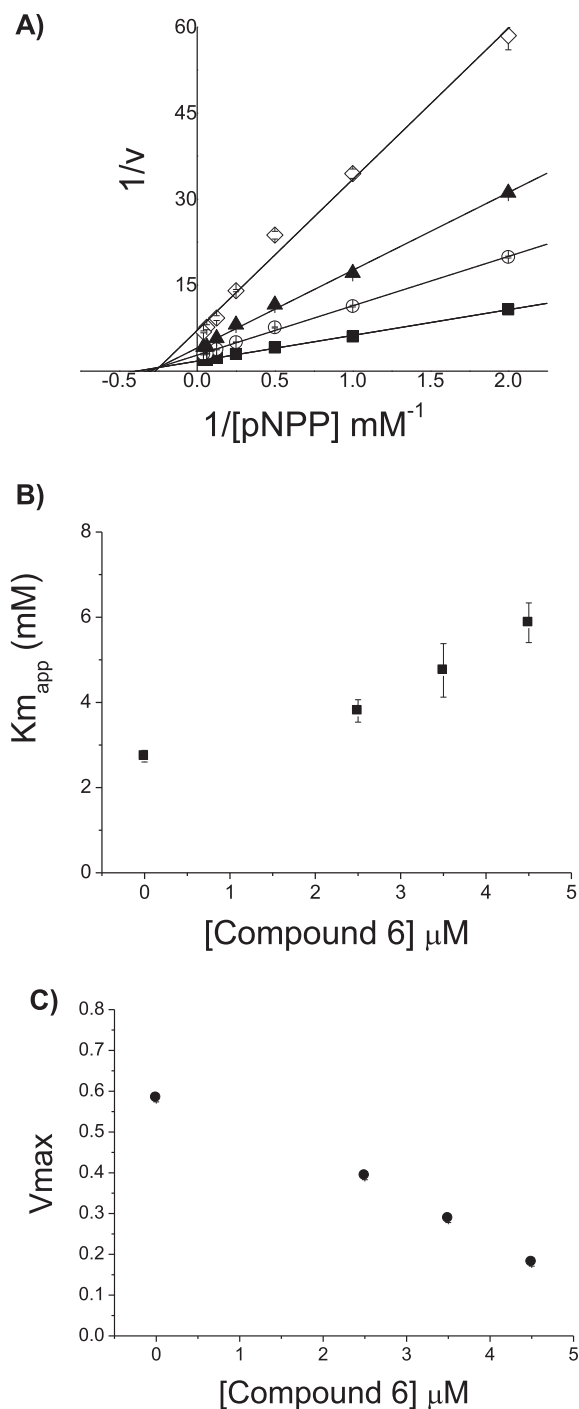
Fig. 4. Inhibition of PTP-1B by compound **6**. Double reciprocal plot of **6** (1/v versus 1/[S]) (A), VdR6 kinetics. The concentration of **6** used were: ■, 0 μM; ○, 2.5 μM; ▲, 3.5 μM; ◇, 4.5 μM. Dependence of main kinetic parameters K_m (B) and V_{max} (C) were determined fitting the values of enzymatic activity calculated at seven different substrate concentration by using a non linear equation fitting program (Fig-Sys) and the Michaelis–Menten equation. The concentration of compound VdR6 used were: 0, 2.5, 3.5 and 4.5 μM. The data reported in the figures represent the value ± S.E.M.

glucose levels (Fig. 6); however, **10** have not shown effect during the first hour of experiment, nevertheless, after 3 h it showed a significant hypoglycaemic effect over 20% similar to that observed for oleanolic acid in previous reports [6]. The performance of **10** during all the experimental time suggests that this compound could be previously metabolized by O-desalkylation given the

oleanolic acid, which is responsible to induce the hypoglycaemic effect. However, several studies are required for such affirmation. On the other hand, **6** induced the most potent and sustained in vivo effect compared with **10**, and also diminished glucose levels below than glibenclamide used as positive control, correlating with in vitro PTP-1B inhibition studies since **6** have shown a mixed enzyme inhibition and low IC_{50}.

2.4. Molecular docking

Docking assays were performed for a better understanding of the interactions between **6** and **10** with PTP-1B. The PTP-1B is an enzyme composed by 435 aminoacid residues, owns a catalytic domain from residue 30 to 278 with some important regions such as the catalytic site (His214-Arg221, were Cys215 is the active nucleophile), WPD loop (Asp181 and Phe182), and pTyr loop (Tyr46-Asp48) [7]. Also, PTP-1B has a secondary binding site (site B) that is catalytically inactive and exposed to cytosol, and the most important residues are Arg24, Arg254, Glu262, Tyr46, Asp48, Val49, Ile219 and Met258 [8]. Using different crystallographic structures, several approaches have been developed to study the interactions between PTP-1B and bioactive molecules, being the most precisely the 2-(oxalylamino)-benzoic acid (Fig. 7) using as crystallographic ligand which allows the study of different regions such as site B [9]. Most studies had focused on improving affinity to the catalytic site still it is highly conserved among phosphatase family, several oleanolic acid derivatives enhance interactions with catalytic site, pTyr and Q loop (Gln262) residues [10].

Previously, it was described that oleanolic acid binds to site B by Van der Waals interactions and hydrogen bridges from C-28 carboxylic acid [6]. In this context, the compounds with higher in vitro inhibitory activity over PTP-1B (**6** and **10**) were docked into PTP-1B (PDB code: 1C83) crystallographic structure, it is important to point out that both compounds have C-3 modifications. As previously discussed, the in vitro evaluation suggest a lost of selectivity of compound **6** on PTP1B, since it showed similar IC_{50} values over all different PTPases. Latter was confirmed by docking assay, where results indicate several Van der Waals interactions with site B residues described previously for oleanolic acid [6], but more important are the hydrophobic interactions with catalytic site through WPD loop (Fig. 8). For **10** various types of interactions were observed (Fig. 9), the most important was the hydrogen bridge between Arg24 residue and C-28 carboxylic acid; others such as Van der Waals type interactions described for oleanolic acid remain unchanged, nevertheless changing the alcohol group in C_3 for ethyl ether, allows a better interaction with WPD loop improving the bond between the enzyme and **10** compared to the original compound.
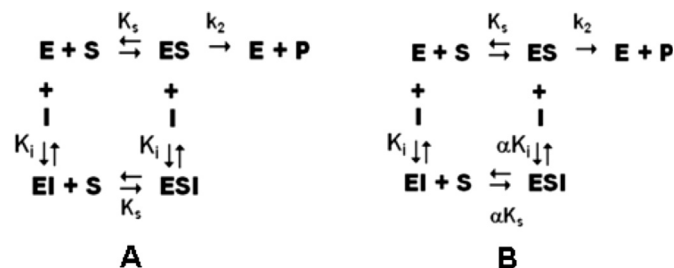
Scheme 2. Inhibition Model: A, noncompetitive; B, mixed. In the scheme: E, free enzyme; ES, enzyme–substrate complex; EI, enzyme–inhibitor complex; ESI, enzyme-substrate-inhibitor ternary complex; P, reaction product.

A)

B)

C)
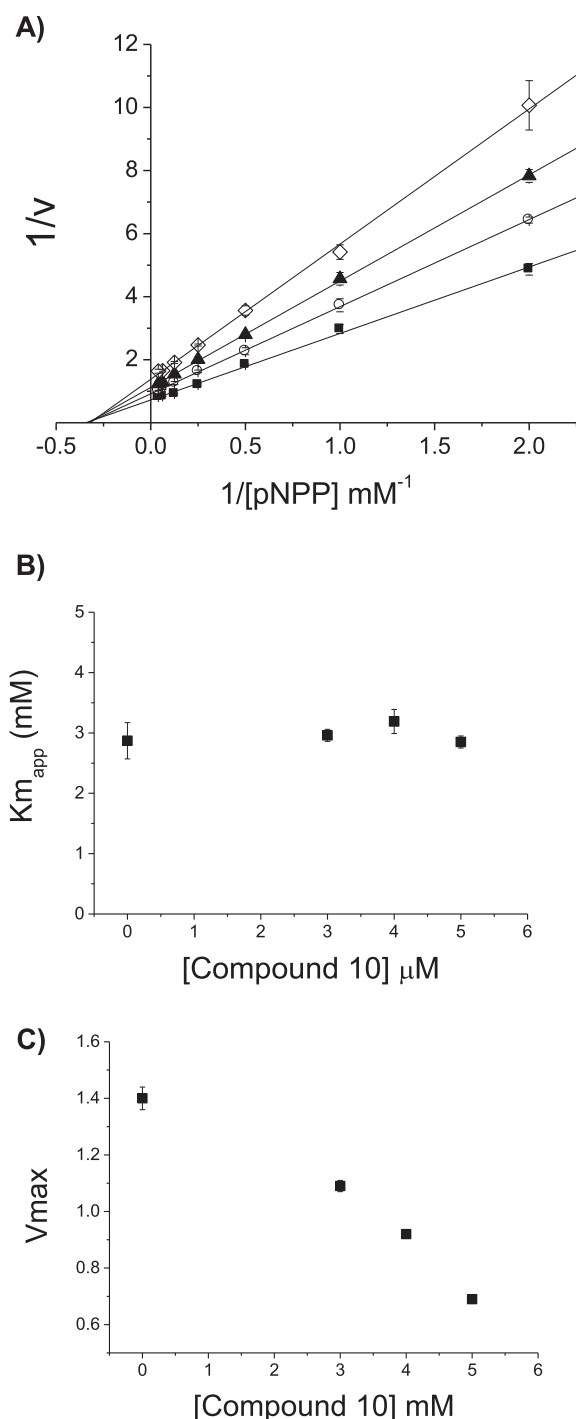
Fig. 5. Inhibition of PTP-1B by compound **10**. Double reciprocal plot of VdR10 (1/v versus 1/[S]) (A), **VdR10** kinetics. The concentration of **10** used were: ■, 0 μM; ○, 3.0 μM; ▲, 4.0 μM; ◊, 5.0 μM. Dependence of main kinetic parameters K_m (B) and V_{max} (C) were determined fitting the values of enzymatic activity calculated at seven different substrate concentration by using a non linear equation fitting program (Fig-Sys) and the Michaelis–Menten equation. The concentration of compound VdR10 used were: 0, 3.0, 4.0 and 5.0 μM. The data reported in the figures represent the value ± S.E.M.

3. Conclusion

During the present investigation, the insulin sensitizing activity of oleanolic acid derivatives was determined, initial screening indicated that the inhibitory activity over PTP-1B was decreased

Table 2
Values of the inhibition constants (Ki), inhibition mechanism and docking scores of compounds **6** and **10**.

| Compound	Inhibition type	Ki (μM)	α	Docking score
Oleanolic acid	Mixed-type	6.0 ± 1.9	2.2	−7.59 kcal/mol
6	Mixed-type	2.1 ± 0.1	1.5	−9.55 kcal/mol
10	Non-competitive	4.8 ± 0.6	–	−6.93 kcal/mol

when the carboxylic acid was replaced by an ester. Moreover, those derivatives on C-3 position had shown the importance of size and type of substituent used. The most active compound was the cinnamoyl ester, even the lack of selectivity due to its union with catalytic site showed important *in vitro* and *in vivo* effects. Furthermore, ethyl ether derivative was the most active compound through *in vitro* studies but it has a similar effect to oleanolic acid, suggesting that this compound is metabolized; however further experiments are necessary to prove this hypothesis.

4. Experimental

4.1. Synthesis of oleanolic acid derivatives

4.1.1. General

The microwave-assisted reactions were carried on in a CEM Discovery BenchMate system with a potency of 100 W and the temperature was established for each reaction under open vessel system. Reactions progress and purity of compounds were monitored by thin layer chromatography (TLC) using pre-coated silica gel 60 F_{254} (250 μm) aluminium sheets, visualizing the plates under UV-light and subsequently spraying with $(NH_4)_4Ce(SO_4)_4$ in 2N H_2SO_4 and heating. All analytical samples were homogeneous on TLC in at least two different solvent systems. Products were purified by flash column chromatography (FCC) using 40–63 μm silica gel (230–440 mesh). All products were solids. Melting points (uncorrected) were determined on a Büchi B-540 apparatus. Optical rotations were measured at room temperature (20–23 °C) on a Perkin–Elmer model 241 polarimeter (concentration in g/100 mL).
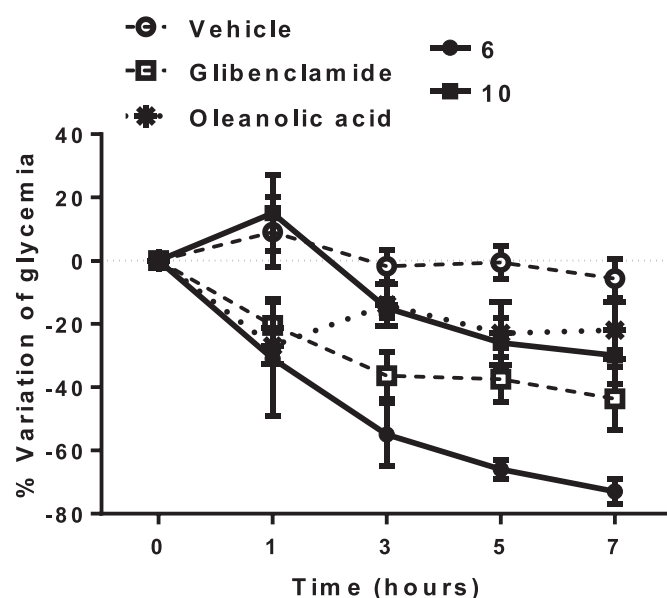
Fig. 6. Acute antidiabetic effect. Diminution of plasmatic glucose concentration over a non-insulin dependent diabetic rat model treated with **6** or **10**. Every point represent the mean ± S.E.M. (*n* = 6).
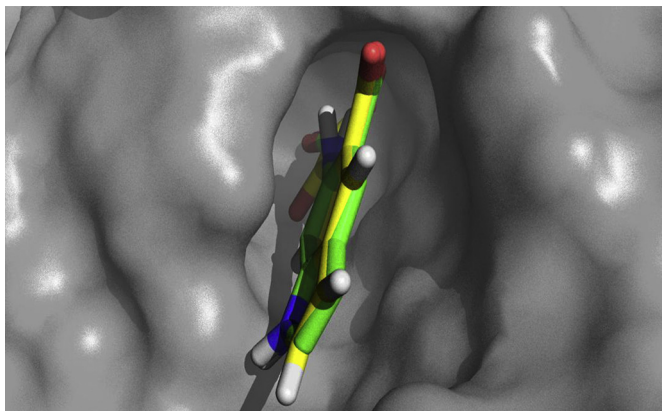
Fig. 7. Docking validation. Representation of the binding site surface of PTP-1B with crystallographic ligand (green) and the position predicted by AutoDock for ligand (yellow). (For the references to colour in this figure, the reader is referred to the electronic version of this article).

IR spectra were recorded in KBr or as films (CHCl$_3$) on a Bruker Vector 22® FT-IR spectrometer. ^{1}H, ^{13}C and 2D NMR experiments were performed (dissolving the samples in 0.5 mL of CDCl$_3$) on a Varian Unity 400® spectrometer, equipped with a 5 mm inverse detection pulse field gradient probe at 25 °C, at 400 MHz for ^{1}H NMR and 100 MHz for ^{13}C NMR. Chemical shifts are given in values of parts per million, referenced to tetramethylsilane (TMS) as an internal standard. A JEOL JMS-700 high-resolution mass spectrometer was used to obtain mass spectrometry data by EIMS$^+$ and HREIMS$^+$.

4.1.2. Chemistry

Oleanolic acid (OA) was purified from the acetone extract of leaves and stems of *Phoradendron brachystachyum* DC Nutt (Viscaceae) as previously reported [11]. Chemical reagents were purchased analytical grade from Sigma–Aldrich, Mexico. Commercially available solvents (*n*-hexane, ethyl acetate and acetone) were used after purification and dried according to standard procedures.

4.1.3. Starting material

Oleanolic acid (OA). TLC: R_f 0.36 (*n*-hexane-acetone 80:20); white needles; m.p. 308–310 °C [Lit. 310 °C] [1]; $[\alpha]^D_{20}$ + 78 (*c* 0.15, CHCl$_3$ [Lit. +60 (*c* 0.01, CHCl$_3$)] [12]; ^{1}H NMR and ^{13}C NMR in accordance with previously reported data for this compound [13].

4.1.4. General procedure for synthesis of compounds 1, 3, 5 and 6

To a well stirred and cooled at 0 °C solution of OA (1.0 equiv.) in dry CH$_2$Cl$_2$ was added dropwise 2.1 equiv. of Et$_3$N. Mixture reaction was stirred at 0 °C for 30 min. Acyl chloride (1.1 equiv.) was added dropwise over a period of 5 min, then mixture reaction was placed under microwave radiation in equipment CEM at 30 °C. Solvent was concentrated under vacuum and de crude reaction was purified by FCC.

4.1.4.1. (3β)-3-(acetyloxy)olean-12-en-28-oic acid (1).
OA (60 mg, 0.13 mmol), CH$_2$Cl$_2$ (5.0 mL), Et$_3$N (270 mg, 40 μL, 0.27 mmol), acetyl chloride (11 mg, 10 μL, 0.14 mmol), 2 h reaction. FCC (*n*-hexane/acetone 97:03 v/v) affording 31 mg product, 48% yield. TLC: R_f 0.51 (*n*-hexane-acetone 80:20); white powder; m.p. 255–257.3 °C [Lit. 258–260 °C]; $[\alpha]^D_{20}$ + 66 (*c* 0.2, CHCl$_3$) [Lit. +28 (*c* 0.05, CHCl$_3$)] [14]; IR (KBr) ν_{max} 3300–2500 (COOH), 2922, 2868, 1727, 1687, 1455, 1363, 1250, 1030, 1009, 802, 746, 647 cm^{-1} [12,14]; ^{1}H NMR and ^{13}C NMR in accordance with previously reported data

for this compound [12,14]; EIMS *m/z*: 410 [M + −COOH−COCH$_3$] (5), 341 (6), 256 (42), 228 (15), 213 (21), 185 (24), 149 (15), 129 (35), 97 (35), 69 (100), 57 (45). HR EIMS *m/z* 498.3636 [M$^+$] (Calculated for C$_{32}$H$_{50}$O$_4$, 498.3709).

4.1.4.2. (3β)-3-(benzoyloxy)olean-12-en-28-oic acid (3).
OA (350 mg, 0.77 mmol), Et$_3$N (160 mg, 230 μL, 1.6 mmol), CH$_2$Cl$_2$ (10.0 mL), benzoyl chloride (118 mg, 100 μL, 0.84 mmol), 5 h reaction. FCC: (*n*-hexane/acetone 83:17 v/v) affording 310 mg product, 72% yield. TLC: R_f 0.48 (*n*-hexane-acetone 80:20); white powder; m.p. 258–260 °C; $[\alpha]^D_{20}$ + 45 (*c* 0.2, CHCl$_3$); UV (λ_{max}, CHCl$_3$): 253 (ε 2050), 259 (ε 1616), 264 (ε 1635), 273 (ε 1897), 279 (ε 1458), 281 (ε 1515); IR (KBr) ν_{max} 3100−2400 (COOH), 2942, 2873, 1713, 1697, 1449, 1272, 1108, 1031, 976, 944, 762, 683 cm^{-1}; ^{1}H NMR (CDCl$_3$, 400 MHz) δ8.05 (2H, dd, *J* = 8.0, 1.6 Hz, H-32, H-36), 7.55 (2H, dt, *J* = 8.0, 1.2 Hz, H-34), 7.44 (1H, dd, *J* = 8.0, 8.0 Hz, H-33, H-35), 5.30 (1H, s, H-12), 4.75 (1H, dd, *J* = 12, 5.6 Hz, H-3), 2.84 (1H, dd, *J* = 14.0, 4.4 Hz, H-18), 2.00 (2H, m, H-11), 1.91 (1H, m, H-15a), 1.78 (1H, m, H-22), 1.77 (1H, m, H-15b), 1.68 (1H, m, H-1a), 1.64 (1H, m, H-19a), 1.62 (1H, m, H-9), 1.59 (2H, m, H-6), 1.58 (1H, m, H-22), 1.36 (1H, m, H-21a), 1.21 (1H, m, H-21b), 1.18 (1H, m, H-19b), 1.16 (3H, m, H-27), 1.16 (1H, m, H-1b), 1.03 (3H, m, H-24), 1.00 (3H, m, H-25), 0.95 (3H, m, H-23), 0.94 (3H, m, H-30), 0.92 (3H, m, H-29), 0.92 (1H, m, H-5), 0.78 (3H, m, H-26); ^{13}C NMR (CDCl$_3$, 100 MHz) δ184.70 (s, C-28), 166.49 (s, C-A), 143.81 (s, C-13), 132.93 (d, C-32, C-36), 131.12 (s, C-31), 129.73 (d, C-34), 128.51 (d, C-33- C-35), 122.73 (d, C-12), 81.75 (d, C-3), 55.54 (d, C-5), 47.75 (d, C-9), 46.75 (s, C-17), 46.02 (t, C-19), 41.74 (s, C-14), 41.05 (d, C-18), 39.48 (s, C-8), 38.29 (t, C-1), 38.02(s, C-4), 37.23 (s, C-10), 33.97 (t, C-21), 33.27 (c, C-29), 32.70 (t, C-7), 32.63 (t, C-22), 30.87 (s, C-20), 28.40 (c, C-3), 27.86 (t, C-2), 26.16 (c, C-27), 23.79 (c, C-30), 23.76 (t, C-15), 23.61 (t, C-11), 23.05 (t, C-16), 18.39 (t, C-6), 17.14 (c, C-24), 17.40 (c, C-26), 15.60 (c, C-25); EIMS *m/z*: 438 [M + −COCH$_3$−CH$_3$-H$_2$] (15), 395 (4), 368 (7), 311 (4), 248 [9] (100), 203 (52), 190 (16), 175 (8), 133 (8), 105 (48), 77 (9), 69 (9). HR EIMS *m/z* 560.3782 [M$^+$] (Calculed for C$_{37}$H$_{52}$O$_4$, 560.3866)

4.1.4.3. (3β)-3-[(2E)-but-2-enoyloxy]olean-12-en-28-oic acid (5).
OA (300 mg, 0.66 mmol), Et$_3$N (14 mg, 19 μL, 1.38 mmol), CH$_2$Cl$_2$ (10.0 mL), crotonoyl chloride (75 mg, 70 μL, 0.72 mmol) 3 h reaction. FCC: (*n*-hexane/acetone 83:17 v/v) affording 71 mg product, 21% yield. TLC: R_f 0.48 (*n*-hexane-acetone 80:20); white powder; m.p. 194.1–196.2 °C; $[\alpha]^D_{20}$ + 45 (*c* 0.1, CHCl$_3$); IR (CHCl$_3$) ν_{max} 3100−2350 (COOH), 2922, 2857, 1715, 1675, 1440, 1303, 1180, 1110, 1007, 957, 912 cm^{-1}; ^{1}H NMR (CDCl$_3$, 400 MHz) δ 6.954 (1H, dq, *J* = 15.2,7.2 Hz, H−C), 5.845 (1H, dd, *J* = 15.6, 2.0 Hz, H−B), 5.27 (1H, dd, *J* = 5.6, 2.8 Hz, H-12), 4.55 (1H, dd, *J* = 9.2, 6.4 Hz, H-3), 2.819 (1H, dd, *J* = 14.0, 4.0 Hz, H-18), 1.88 (1H, m, H-11a), 1.88 (3H, dd, *J* = 6.4,1.2 Hz, H-D), 1.74 (1H, m, H-22), 1.64 (1H, m, H-11b), 1.63 (1H, m, H-19a), 1.61 (1H, m, H-1a), 1.57 (1H, m, H-9), 1.56 (1H, m, H-22), 1.53 (1H, m, H-6a), 1.43 (1H, m, H-7a), 1.37 (1H, m, H-6b), 1.35 (1H, m, H-21a), 1.28 (1H, m, H-7b), 1.21 (1H, m, H-21b), 1.14 (1H, m, H-19b), 1.13 (3H, s, H-27), 1.06 (2H, m, H-2), 1.06 (1H, m, H-1b), 1.02 (1H, m, H-15a), 0.96 (2H, m, H-16), 0.95 (3H, s, H-25), 0.94 (1H, m, H-15b), 0.93 (3H, s, H-30), 0.91 (3H, s, H-29), 0.88 (3H, s, H-24), 0.87 (3H, s, H-23), 0.855 (1H, m, H-5), 0.75 (3H, s, H-26); ^{13}C NMR (CDCl$_3$, 100 MHz) δ 184.41 (s, C-28), 166.64 (s, C-A), 144.37 (d, C−C), 143.79 (s, C-13), 123.49 (d, C−3B), 122.73 (d, C-12), 80.72 (d, C-3), 55.47 (d, C-5), 47.72 (d, C-9), 46.72 (s, C-17), 46.01 (t, C-19), 41.72 (s, C-14), 41.08 (d, C-18), 39.45 (s, C-8), 38.23 (t, C-1), 38.02(s, C-4), 37.17 (s, C-10), 33.97 (t, C-21), 33.27 (c, C-29), 32.69 (t, C-7), 32.62 (t, C-22), 30.87 (s, C-20), 28.26 (c, C-23), 27.85 (t, C-2, C-15, 26.12 (c, C-27), 23.78 (c, C-30), 23.58 (t, C-11), 23.05 (t, C-16), 18.36 (t, C-6), 18.16 (c, C-D), 17.34 (c, C-26), 16.96 (c, C-24), 15.61 (c, C-25; EIMS *m/z*: 438 [M + -COCH3-CH3-H2] (3), 287 (83), 248 [9] (16), 203 (13), 102

A

B

C
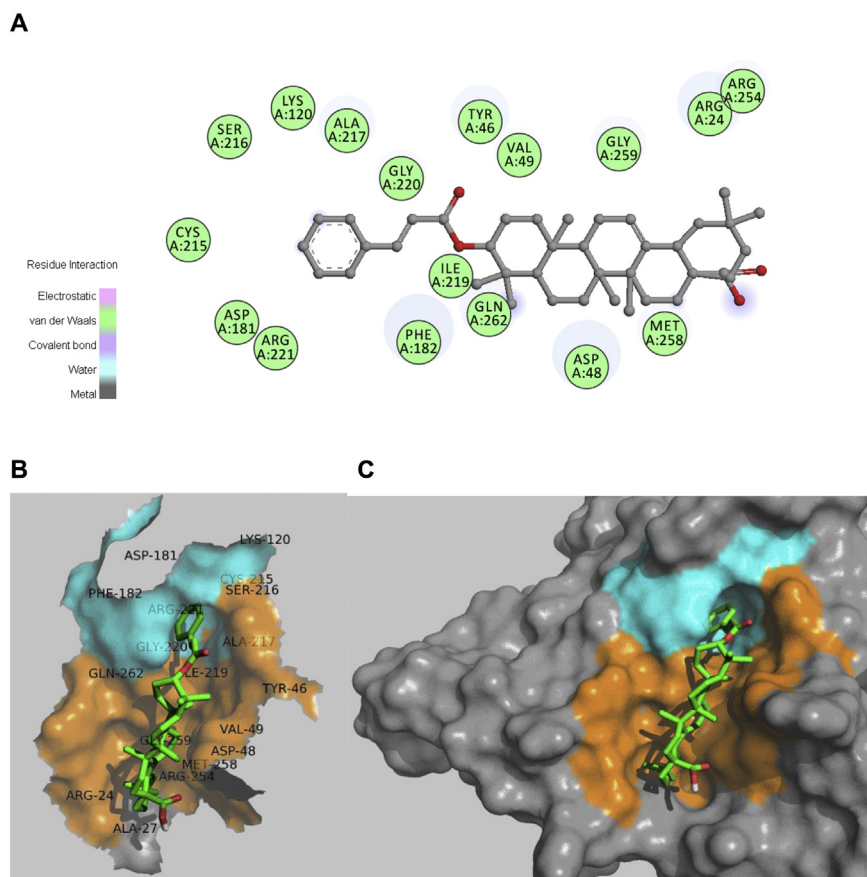
Fig. 8. Docking of 6. A) Two-dimensional interaction diagram of the predicted binding mode of **6**. Van Der Waals residues are represented in green. B) Three-dimensional binding model of **6** showing interaction with both site B and catalytic site residues. C) Surface representation of PTP-1B showing the binding mode of **6** in the binding site B (orange) and interactions with the catalytic site (blue). (For the references to colour in this figure, the reader is referred to the electronic version of this article).

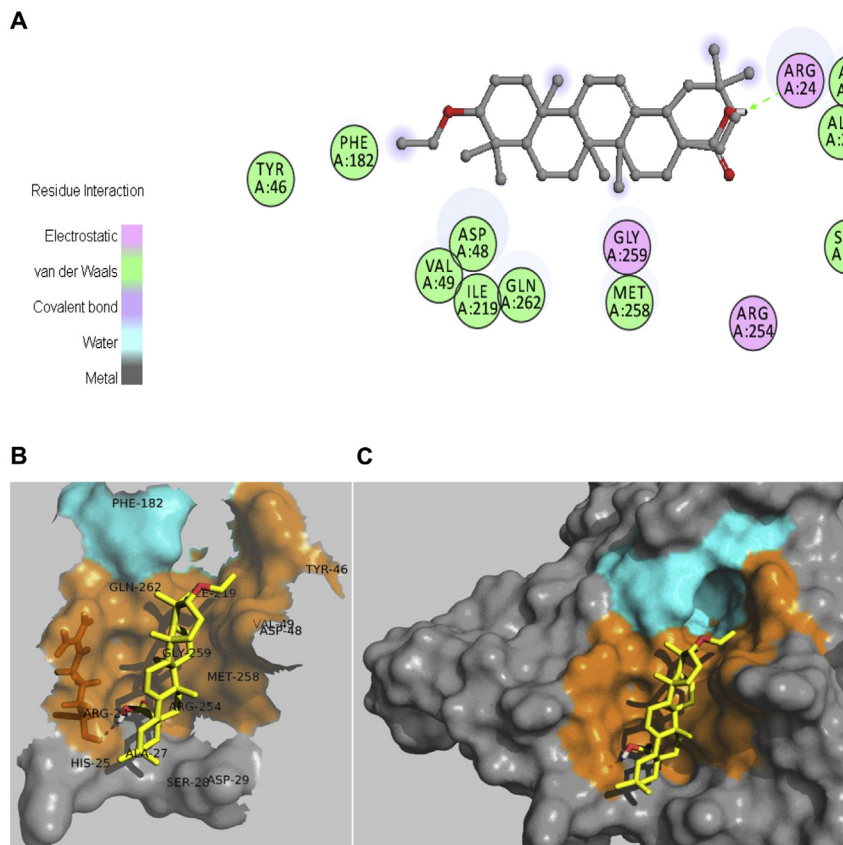(100). HR EIMS m/z 524.3810 [M$^+$] (Calculed for $C_{34}H_{52}O_4$, 524.3866)

4.1.4.4. (3β)-3-{[(2E)-3-phenylprop-2-enoyl]oxy}olean-12-en-28-oic acid (**6**). OA (300 mg, 0.66 mmol), Et$_3$N (140 mg, 200 μL, 1.38 mmol), CH$_2$Cl$_2$ (10 mL), cinnamoyl chloride (120 mg, 0.72 mmol) 1.5 h reaction. FCC: (n-hexane/acetone 95:05 v/v) affording 173 mg product, 45% yield. TLC: R_f 0.45 (n-hexane-acetone 80:20); white powder; m.p. 272–274.5 °C; [α]$^D_{20}$ + 28 (c 0.1, CHCl$_3$); IR (CHCl$_3$) ν_{max} 3100−2400 (COOH), 2942, 1706, 1636, 1450, 1305, 1257, 1165, 1015, 970, 799, 774 cm^{-1}; ^{1}H NMR (CDCl$_3$, 400 MHz) δ 7.67 (1H, d, J = 16.0 Hz, H−C), 7.53 (1H, dd, J = 7.6, 3.6 Hz, H-32, H-36), 7.38 (3H, m, H-33, H-34, H-35), 6.45 (1H, d, J = 16.0 Hz, H−B), 5.28 (1H, dd, J = 3.2, 3.2 Hz, H-12), 4.65 (1H, dd, J = 8.8, 7.6 Hz, H-3), 2.83 (1H, dd, J = 13.6, 4.0 Hz, H-18), 2.10 (1H, m, H-16a), 1.98 (1H, m, H-16b),1.89 (1H, m, H-11a), 1.77 (1H, m, H-22), 1.71 (1H, m, H-11b),1.65 (1H, m, H-1a), 1.64 (1H, m, H-19a), 1.60 (1H, m, H-9), 1.57 (1H, m, H-22), 1.55 (1H, m, H-6a), 1.38 (1H, m, H-6b),1.38 (1H, m, H-21a), 1.35 (1H, m, H-21b), 1.18 (1H, m, H-19b), 1.14 (3H, m, H-27), 1.10 (1H, m, H-1b), 0.98 (3H, m, H-25), 0.94 (3H, m, H-24), 0.93 (3H, m, H-30), 0.92 (3H, m, H-23), 0.91 (3H, m, H-29), 0.88 (1H, m, H-5), 0.76 (3H, m, H-26); ^{13}C NMR (CDCl$_3$, 100 MHz) δ 184.76 (s, C-28), 167.06 (s, C-A), 144.53 (d, C−C), 143.79 (s, C-13), 134.67 (s, C-31), 130.35 (d, C-32, C-36), 129.04 (d, C-34), 128.23 (d, C-33, C-35), 122.72 (d, C-12), 118.94 (d, C−B), 81.75 (d, C-3), 55.54 (d, C-5), 47.72 (d, C-9), 46.72 (s, C-17), 45.99 (t, C-19), 41.69 (s, C-14), 41.01 (d, C-18), 39.44 (s, C-8), 38.23 (t, C-1), 38.12(s, C-4), 37.18 (s, C-10), 33.94 (t, C-21), 33.27 (c, C-29), 32.66 (t, C-7), 32.61 (t, C-22), 30.86 (s, C-20), 28.29 (c, C-23), 27.84 (t, C-2), 26.14 (c, C-27), 23.83 (t, C-11), 23.81 (t, C-15), 23.78 (c, C-30), 23.01 (t, C-16), 18.36 (t, C-6), 17.38 (c, C-26), 17.02 (c, C-24), 15.60 (c, C-25); EIMS m/z: 248 [15] (15), 203 (19), 147 (11), 131 (100), 103 (22), 69 (8). HR CIMS [M + H]$^+$ 587.4067 [M + H]$^+$ (Calculated for $C_{39}H_{55}O_4$, 587.4022).

4.1.5. General procedure for synthesis of compounds **2**, **4** and **7**

OA (1.0 equiv.) and K$_2$CO$_3$ (1.1 equiv.) were dissolved in dry CHCl$_3$/DMF (3:1 v/v). Solution was stirred at 0 °C for 15 min. Alkyl halide (2.1 equiv.) was added dropwise over a period of 5 min, then mixture reaction was placed under microwave radiation in equipment CEM at 60 °C. Solvent was concentrated under vacuum and de crude reaction was purified by FCC.

4.1.5.1. Methyl (3β)-3-hydroxyolean-12-en-28-oate (**2**). OA (300 mg, 0.66 mmol), K$_2$CO$_3$ (100 mg, 0.72 mmol), CHCl$_3$/DMF (4 mL), iodomethane (200 mg, 100 μL, 1.38 mmol), 2.5 h reaction. FCC: (n-hexane/acetone 95:05 v/v) affording 232 mg product, 75% yield. TLC: R_f 0.42 (n-hexane-acetone 80:20); white powder; m.p. 164–167 °C; [α]$^D_{20}$ + 17 (c 0.2, CHCl$_3$); IR (CHCl$_3$) ν_{max} 2928, 2859, 1720, 1464, 1387, 1263, 1188, 1159, 1032, 997, 751 cm^{-1}; ^{1}H NMR (CDCl$_3$, 400 MHz) δ 5.28 (1H, dd, J = 3.2, 3.2 Hz, H-12), 3.62 (3H, s, H-A), 3.25 (1H, dd, J = 10.8, 4.4 Hz, H-3), 2.86 (1H, dd, J = 14.0, 4.0 Hz, H-18), 2.05 (1H, m, H-11a), 2.00 (1H, m, H-11b), 1.75 (2H, m, H-7), 1.62 (1H, m, H-1a), 1.60 (1H, m, H-22), 1.60 (1H, m, H-6a), 1.57 (1H, m, H-6b), 1.55 (1H, m, H-9), 1.53 (2H, m, H-21), 1.38 (1H, m, H-22), 1.18 (2H, m, H-19), 1.13 (3H, s, H-27), 0.99 (3H, s, H-23), 0.94 (3H, s, H-30), 0.92 (1H, m, H-1b), 0.90 (3H, s, H-25), 0.90 (3H, s, H-29), 0.78

A

Residue Interaction

Electrostatic

van der Waals

Covalent bond

Water

Metal

B   **C**

Fig. 9. Docking of 10. A) Two-dimensional interaction diagram of the predicted binding mode of **10**. Residues are represented by colour as follows: electrostatic residues in pink and Van Der Waals residues in green. B) Three-dimensional binding model of VdR10 showing interaction with site B residues. C) Surface representation of PTP-1B showing the binding mode of **10** in the binding site B (orange) and absence of interactions with the catalytic site (blue). (For the references to colour in this figure, the reader is referred to the electronic version of this article.)

(3H, s, H-24), 0.77 (1H, m, H-5), 0.72 (3H, s, H-26); ^{13}C NMR (CDCl$_3$, 100 MHz) δ 178.52 (s, C-28), 143.95 (s, C-13), 122.53 (d, C-12), 79.20 (d, C-3), 55.39 (d, C-5), 51.75 (c, C-A), 47.80 (d, C-9), 46.90 (s, C-17), 46.05 (t, C-19), 41.80 (s, C-8), 41.45 (d, C-18), 39.34 (s, C-14), 38.94(s, C-4), 38.61 (t, C-1), 37.21 (s, C-10), 34.03 (t, C-22), 33.31 (c, C-29), 32.83 (t, C-21), 32.56 (t, C-7), 30.89 (s, C-20), 28.29 (c, C-23), 27.88 (t, C-2), 27.35 (t, C-15), 26.13 (c, C-27), 23.85 (c, C-30), 23.59 (t, C-11), 23.25 (t, C-16), 18.52 (t, C-6), 17.02 (c, C-26), 15.78 (c, C-24), 15.50 (c, C-25). EIMS m/z: 470 [M+] (8), 262 (70), 203 (100), 202 (24), 175 (9), 133 (12), 119 (11), 81 (11), 60 (13), 55 (7). HR EIMS m/z 470.3738 [M$^+$] (Calculated for C$_{31}$H$_{50}$O$_3$, 470.3760)

4.1.5.2. Ethyl (3β)-3-hydroxyolean-12-en-28-oate (**4**).

OA (300 mg, 0.66 mmol), K$_2$CO$_3$ (100 mg, 0.72 mmol), CHCl$_3$/DMF (4 mL), bromoethane (150 mg, 100 µL, 1.38 mmol), 2 h reaction. FCC: (n-hexane/acetone 95:05 v/v) affording 163 mg product, 51% yield. TLC: R_f 0.51 (n-hexane-acetone 80:20); white powder; m.p. 175–177; $[\alpha]^D_{20}$ + 10.16 (c 0.2, CHCl$_3$); IR (CHCl$_3$) ν_{max} 3280, 2932, 2867, 1715, 1463, 1387, 1360, 1252, 1182, 1160, 1032, 995, 754 cm^{-1}; ^{1}H NMR (CDCl$_3$, 400 MHz) δ 5.28 (1H, dd, J = 3.2,3.2 Hz, H-12), 4.09 (1H, cd, J = 7.2, 3.2 Hz, H-Aa), 4.07 (1H, cd, J = 7.2,3.2 Hz, H-Ab), 3.21 (1H, dd, J = 10.8,4.4 Hz, H-3), 2.87 (1H, dd, J = 14,4.4 Hz, H-18), 1.96 (1H, m, H-11a), 1.95 (1H, ddd, J = 13.6,13.6,4.8 Hz, H-16a), 1.87 (1H, m, H-16b), 1.68 (1H, m, H-7a), 1.64 (1H, m, H-19a), 1.61 (3H, m, H-11b, H-15), 1.60 (1H, m, H-1a), 1.52 (3H, m, H-9, H-6), 1.51 (1H, m, H-7b), 1.34 (1H, m, H-21a), 1.23 (3H, t, J = 7.2 Hz, H–B), 1.18 (1H, m, H-21b), 1.15 (1H, m, H-19b), 1.13 (3H, s, H-27), 0.98 (3H, s, H-23), 0.96 (1H, m, H-1b), 0.92 (3H, s, H-30), 0.90 (3H, s, H-29), 0.89 (3H, s, H-25), 0.78 (3H, s, H-24), 0.74 (3H, s, H-26), 0.73 (1H, m, H-5); ^{13}C NMR (CDCl$_3$,

100 MHz) δ 177.94 (s, C-28), 143.93 (s, C-13), 122.44 (d, C-12), 79.15 (d, C-3), 60.28 (t, C-A), 55.35 (d, C-5), 47.77 (d, C-9), 46.64 (s, C-17), 46.05 (t, C-19), 41.84 (s, C-8), 41.42 (d, C-18), 39.47 (s, C-14), 38.91 (s, C-4), 38.59 (t, C-1), 37.17 (s, C-10), 34.05 (t, C-21), 33.31 (c, C-29), 32.56 (t, C-7), 32.89 (t, C-22), 30.88 (s, C-20), 28.27 (c, C-23), 27.79 (t, C-2), 27.32 (t, C-15), 26.03 (c, C-27), 23.80 (c, C-30), 23.57 (t, C-16), 23.14 (t, C-11), 18.49 (t, C-6), 17.13 (c, C-26), 15.78 (c, C-24), 15.49 (c, C-25), 14.46 (c, C–B); EIMS m/z: 484 [M+] (12), 411 (13), 410 (12), 276 (45), 203 (100), 189 (30), 145 (15), 119 (26), 81 (27), 69 (52), 57 (30). HR EIMS m/z 484.3899 [M$^+$] (Calculated for C$_{33}$H$_{52}$O$_3$, 484.3919).

4.1.5.3. Benzyl (3β)-3-hydroxyolean-12-en-28-oate (**7**).

OA (300 mg, 0.66 mmol), K$_2$CO$_3$ (100 mg, 0.72 mmol), CHCl$_3$/DMF (4 mL), benzyl chloride (175 mg, 160 µL, 1.38 mmol), 3 h reaction. FCC: (n-hexane/acetone 90:10 v/v) affording 275 mg product, 76.4% yield. TLC: R_f 0.42 (n-hexane-acetone 80:20); white powder; m.p. 188–190 [Lit. 190–192 °C] [4]; $[\alpha]^D_{20}$ + 47 (c 0.2, CHCl$_3$) [Lit. +50.1 (c 2.44, CHCl$_3$)] [11]; IR (CHCl$_3$) ν_{max} 3578, 2936, 2920, 2864, 1723, 1464, 1448, 1384, 1375, 1183, 1161, 1129, 1038, 1011, 995 cm^{-1}; ^{1}H NMR and ^{13}C NMR in accordance with previously reported data for this compound [13]; EIMS m/z: 546 [M+] (4), 437 (26), 411 (8), 338 (7), 247 (20), 203 (26), 201 (22), 91 (100). HR EIMS m/z 546.4090 [M$^+$] (Calculated for C$_{37}$H$_{54}$O$_3$, 546.4073).

4.1.6. General procedure for the synthesis of compounds **9**, **10** and **11**

To a well stirred and cooled at 0 °C solution of OA (1.0 equiv.) in dry THF/DMF (3:1 v/v) was added metallic sodium (2.5 equiv.

washed with hexane and absolute ethanol). Mixture reaction was stirred at 0 °C for 30 min. Alkyl halide (2.1 equiv.) was added dropwise over a period of 5 min, then mixture reaction was placed under microwave radiation in equipment CEM at 50 °C. Solvent was concentrated under vacuum and de crude reaction was purified by FCC.

4.1.6.1. (3β)-3-methoxyolean-12-en-28-oic acid (9). OA (200 mg, 0.44 mmol), Na (25 mg, 1.09 mmol), THF/DMF (6 mL), iodomethane (130 mg, 60 μL, 0.92 mmol), 1 h reaction. FCC: (*n*-hexane/AcOEt 90:10 v/v) affording 125 mg product, 61% yield. TLC: R_f 0.48 (*n*-hexane-AcOEt 80:20); white powder; m.p. 194–197; OR $[\alpha]^D_{20}$ + 96 (*c* 0.2, CHCl$_3$); IR (CHCl$_3$) ν_{max} 3337, 2941, 2925, 2864, 1715, 1458, 1384, 1188, 1161, 1127, 1030, 993, 907, 740, 657 cm^{-1}; ^{1}H NMR (CDCl$_3$, 400 MHz) δ 5.28 (1H, *m*, H-12), 3.62 (3H, *s*, H-A), 3.21 (1H, *dd*, *J* = 10.8, 5.2 Hz, H-3), 2.86 (1H, *dd*, *J* = 14.0, 4.4 Hz, H-18), 2.00 (1H, *m*, H-16a), 1.88 (2H, *m*, H-11), 1.72 (1H, *m*, H-22a), 1.70 (2H, *m*, H-15), 1.65 (1H, *m*, H-19a), 1.63 (1H, *m*, H-16b), 1.60 (1H, *m*, H-1a), 1.59 (2H, *m*, H-2), 1.55 (1H, *m*, H-6a), 1.54 (1H, *m*, H-9), 1.53 (1H, *m*, H-22b),1.49 (1H, *m*, H-7a), 1.40 (1H, *m*, H-6b), 1.32 (1H, *m*, H-21a), 1.29 (1H, *m*, H-7b), 1.28 (1H, *m*, H-22), 1.19 (1H, *m*, H-21b), 1.14 (1H, *m*, H-19b), 1.12 (3H, *s*, H-27), 0.98 (3H, *s*, H-23),0.96 (1H, *m*, H-1b), 0.93 (3H, *s*, H-30), 0.91 (3H, *s*, H-25), 0.89 (3H, *s*, H-29), 0.78 (3H, *s*, H-24), 0.74 (1H, *m*, H-5), 0.71 (3H, *s*, H-26); ^{13}C NMR (CDCl$_3$, 100 MHz) δ 178.50 (*s*, C-28), 144.00 (*s*, C-13), 122.58 (*d*, C-12), 79.24 (*d*, C-3), 55.46 (*d*, C-5), 51.73 (*c*, C-A), 47.86 (*d*, C-9), 46.95 (*s*, C-17), 46.11 (*t*, C-19), 41.87 (*s*, C-14), 41.53 (*d*, C-18), 39.51 (*s*, C-8), 38.98 (*t*, C-1), 38.98(*s*, C-4), 38.67 (*s*, C-10), 34.30 (*t*, C-21), 33.30 (*c*, C-29), 33.30 (*t*, C-22), 33.30 (*t*, C-7), 30.91 (*s*, C-20), 28.86 (*t*, C-15), 28.32 (*c*, C-23), 27.96 (*t*, C-2), 26.16 (*c*, C-27), 23.80 (*c*, C-30), 23.63 (*t*, C-11), 23.30 (*t*, C-16), 18.56 (*t*, C-6), 17.06 (*c*, C-26), 15.79 (*c*, C-24), 15.52 (*c*, C-25); EIMS *m/z*: 470 [M+] (9), 262 (70), 203 (100), 202 (28), 187 (24), 133 (15), 119 (15), 84 (42), 69 (12), 57 (11). HR CIMS [M + H]$^+$ 471.3815 [M + H]$^+$ (Calculated for C$_{31}$H$_{51}$O$_3$, 471.3760).

4.1.6.2. (3β)-3-ethoxyolean-12-en-28-oic acid (10). OA (250 mg, 0.55 mmol), Na (30 mg, 1.37 mmol), THF/DMF (6 mL), bromoethane (125 mg, 90 μL, 1.15 mmol), 2 h reaction. FCC: (*n*-hexane/AcOEt 90:10 v/v) affording 160 mg product, 60% yield. TLC: R_f 0.62 (*n*-hexane-AcOEt 80:20); white powder; m.p. 157.3–159.7 $[\alpha]^D_{20}$ + 67 (*c* 0.2, CHCl$_3$). IR (CHCl$_3$) ν_{max} 3300−2600 (COOH), 2938, 2973, 1722, 1682, 1459, 1381, 1361, 1183, 1110, 1075, 825, 732 cm^{-1}; ^{1}H NMR (CDCl$_3$, 400 MHz) δ 5.27 (1H, *dd*, *J* = 3.2, 3.2 Hz, H-12), 3.66 (1H, *cd*, *J* = 6.8, 2.4 Hz, H-A), 3.35 (1H, *cd*, *J* = 6.8, 2.4 Hz, H-A), 2.82 (1H, *dd*, *J* = 13.6, 4.8 Hz, H-18), 2.75 (1H, *m*, H-3), 1.97 (1H, *ddd*, *J* = 13.6, 13.6, 4.0 Hz, H-15a), 1.88 (2H, *m*, H-11), 1.78 (1H, *m*, H-16a), 1.76 (1H, *m*, H-7a), 1.72 (1H, *m*, H-2a), 1.70 (1H, *m*, H-15b), 1.64 (1H, *m*, H-19a), 1.63 (1H, *m*, H-1a), 1.54 (1H, *m*, H-7a), 1.54 (1H, *m*, H-9), 1.53 (1H, *m*, H-16b), 1.51 (1H, *m*, H-6a), 1.43 (H, *m*, H-22a), 1.33 (1H, *m*, H-21a), 1.39 (1H, *m*, H-6b), 1.28 (H, *m*, H-22b), 1.21 (1H, *m*, H-21b), 1.17 (3H, *t*, *J* = 6.8 Hz, H−B), 1.15 (1H, *m*, H-19b), 1.11 (3H, *s*, H-27), 1.08 (1H, *m*, H-2b), 0.95 (3H, *s*, H-23), 0.91 (1H, *m*, H-1b), 0.91 (3H, *s*, H-30), 0.90 (3H, *s*, H-25), 0.89 (3H, *s*, H-29), 0.77 (3H, *s*, H-24), 0.74 (3H, *s*, H-26), 0.74 (1H, *m*, H-5); ^{13}C NMR (CDCl$_3$, 100 MHz) δ 184.42 (*s*, C-28), 143.82 (*s*, C-13), 122.92 (*d*, C-12), 86.96 (*d*, C-3), 65.41 (*t*, C-A), 56.05 (*d*, C-5), 47.89 (*d*, C-9), 46.77 (*s*, C-17), 46.13 (*t*, C-19), 41.78 (*d*, C-18), 41.13 (*s*, C-14), 39.55 (*s*, C-8), 38.91(*s*, C-4), 38.69 (*t*, C-1), 37.29 (*s*, C-10), 34.03 (*t*, C-21), 33.29 (*c*, C-29), 32.85 (*t*, C-22), 32.67 (*t*, C-7), 30.88 (*s*, C-20), 28.39 (*c*, C-23), 27.91 (*t*, C-2), 26.17 (*c*, C-27), 23.81 (*c*, C-30), 23.67 (*t*, C-11), 23.40 (*t*, C-16), 23.13 (*t*, C-15), 18.49 (*t*, C-6), 17.41 (*c*, C-26), 16.65 (*c*, C-24), 15.87 (*c*, C−B), 15.54 (*c*, C-25); EIMS *m/z*: 484 [M+] (10), 424 (19), 411 (13), 276 (33), 248 [retro Diel-s−Alder] (64), 203 (100), 189 (22), 175 (11), 133 (11), 119 (10), 95 (11), 69 (12), 57 (9). HR CIMS [M + H]$^+$ 485.3904 [M + H]$^+$ (Calculated for C$_{32}$H$_{53}$O$_3$, 485.3916).

4.1.6.3. (3β)-3-propoxyolean-12-en-28-oic acid (11). OA (300 mg, 0.66 mmol), Na (37 mg, 1.65 mmol), THF/DMF (6 mL), 1-iodopropane (240 mg, 140 μL, 1.41 mmol) 3.5 h reaction. FCC: (*n*-hexane/AcOEt 90:10 v/v) affording 118 mg product, 36% yield. TLC: R_f 0.57 (*n*-hexane-AcOEt 80:20); white powder; m.p. 150−153. $[\alpha]^D_{20}$ + 77 (*c* 0.2, CHCl$_3$). IR (CHCl$_3$) ν_{max} 3394, 2945, 2858, 1717, 1460, 1381, 1251, 1158, 1028, 997, 937, 748, 667 cm^{-1}; ^{1}H NMR (CDCl$_3$, 400 MHz) δ 5.28 (1H, *dd*, *J* = 3.2, 3.2 Hz, H-12), 4.00 (1H, *cd*, *J* = 6.8, 2.4 Hz, H-Aa), 3.95 (1H, *cd*, *J* = 6.8, 2.4 Hz, H-Ab), 3.21 (1H, *dd*, *J* = 10.8, 4.8 Hz, H-3), 2.75 (1H, *dd*, *J* = 14.0,4.8 Hz, H-18), 1.98 (1H, *m*, H-16a), 1.85 (1H, *m*, H-16b), 1.62 (2H, *m*, H-11), 1.71 (1H, *m*, H-7a), 1.65 (1H, *m*, H-19a), 1.61 (1H, *m*, H-1a), 1.59 (2H, *m*, H-15b), 1.54 (1H, *m*, H-7a), 1.51 (2H, *m*, H-9), 1.52 (2H, *m*, H-6), 1.34 (1H, *m*, H-21a), 1.18 (1H, *m*, H-21b), 1.16 (1H, *m*, H-19b), 1.13 (3H, *s*, H-27), 0.99 (3H, *s*, H-23), 0.96 (2H, *t*, *J* = 7.6 Hz, H−B), 0.94 (3H, *t*, *J* = 7.6 Hz, H−C), 0.95 (1H, *m*, H-1b), 0.92 (3H, *s*, H-30), 0.91 (3H, *s*, H-25), 0.90 (3H, *s*, H-29), 0.77 (3H, *s*, H-24), 0.74 (3H, *s*, H-26), 0.72 (1H, *m*, H-5); ^{13}C NMR (CDCl$_3$, 100 MHz) δ 176.53 (*s*, C-28), 144.81 (*s*, C-13), 122.22 (*d*, C-12), 79.19 (*d*, C-3), 65.78 (*t*, C-A), 55.87 (*d*, C-5), 47.78 (*d*, C-9), 46.92 (*s*, C-17), 46.04 (*t*, C-19), 41.54 (*d*, C-18), 39.44 (*s*, C-14), 41.86 (*s*, C-8), 38.93 (*s*, C-4), 38.61 (*t*, C-1), 37.18 (*s*, C-10), 34.03 (*t*, C-21), 33.31 (*c*, C-29), 32.88 (*t*, C-7), 32.52 (*t*, C-22), 30.90 (*s*, C-20), 28.29 (*c*, C-23), 27.80 (*t*, C-2), 27.37 (*t*, C-15), 26.08 (*c*, C-27), 23.85 (*c*, C-30), 23.58 (*t*, C−B), 23.23 (*t*, C-11), 18.50 (*t*, C-6), 17.06 (*c*, C-26), 15.79 (*c*, C-24), 15.50 (*c*, C-25), 10.79 (*c*, C−C); EIMS *m/z*: 498 [M+] (18), 411 (22), 410 (21), 290 (65), 203 (100), 189 (25), 119 (9), 105 (8). HR EIMS *m/z* 498.4042 [M$^+$] (Calculated for C$_{33}$H$_{54}$O$_3$, 498.4073).

4.1.7. (3β)-olean-12-ene-3,28-diol (8)

To a cooled (0 °C) solution of LiAlH$_4$ (100 mg, 2.63 mmol) in dry THF (10 mL) was added dropwise OA (300 mg, 0.66 mmol) in dry THF (5 mL) under N$_2$ atmosphere. Suspension was stirred at 0 °C for 1 h, allowed to rise to room temperature and kept for 30 min. Mixture reaction was refluxed 8 h and then stirred at room temperature overnight. Reaction was quenched by addition of a mixture of 2 mL of H$_2$O distilled and 5 mL of NaOH 10%, stirring 1 h. Precipitate was filtered and washed with ethyl acetate (3 × 5 mL). Organic phase was separated and aqueous layer was further extracted with ethyl acetate (3 × 5 mL). Combined organic phases were dried over anhydrous Na$_2$SO$_4$ and evaporated under reduced pressure. FCC: (*n*-hexane/acetone 90:10 v/v) affording 175 mg product, 60% yield. TLC: R_f 0.41 (*n*-hexane-acetone 80:20); yellow powder; m.p. 201−204 [Lit. 229 °C]; $[\alpha]^D_{20}$ + 76 (*c* 0.2, CHCl$_3$) [Lit. +41 (*c* 0.6, MeOH)] [16]; IR (CHCl$_3$) ν_{max} 3329, 2920, 2856, 1710, 1464, 1389, 1359, 1094, 1044, 1006 cm^{-1}; ^{1}H NMR (CDCl$_3$, 400 MHz) δ 5.19 (1H, *dd*, *J* = 3.6, 3.6 Hz, H-12), 3.57 (1H, *d*, *J* = 11.2 Hz, H-28a), 3.23 (1H, *dd*, *J* = 11.2, 4.4Hz, H-3), 3.22 (1H, *d*, *J* = 11.2 Hz, H-28b), 1.99 (1H, *m*, H-18), 1.98 (1H, *m*, H-16a), 1.87 (1H, *m*, H-16b), 1.76 (1H, *m*, H-19a), 1.74 (2H, *m*, H-2), 1.63 (1H, *m*, H-1a), 1.61 (2H, *m*, H-15), 1.56 (2H, *m*, H-6), 1.55 (1H, *m*, H-9), 1.53 (1H, *m*, H-22), 1.53 (1H, *m*, H-7a), 1.33 (2H, *m*, H-21), 1.32 (1H, *m*, H-22), 1.30 (1H, *m*, H-7b), 1.18 (2H, *m*, H-11), 1.16 (3H, *s*, H-27), 1.08 (1H, *m*, H-19b), 0.99 (3H, *s*, H-23), 0.97 (1H, *m*, H-1b), 0.94 (3H, *s*, H-26), 0.93 (3H, *s*, H-24), 0.89 (3H, *s*, H-29), 0.87 (3H, *s*, H-30), 0.79 (3H, *s*, H-25), 0.74 (1H, *m*, H-5); ^{13}C NMR (CDCl$_3$, 100 MHz) δ (multiplicity and assignment) 144.37 (*s*, C-13), 122.50 (*d*, C-12), 79.19 (*d*, C-3), 69.85 (*t*, C-28), 55.31 (d, C-5), 47.73 (*d*, C-9), 46.62 (*t*, C-19), 46.04 (*s*, C-17), 42.50 (*d*, C-18), 41.87 (*s*, C-8), 39.93 (*s*, C-14), 38.94 (*s*, C-4), 38.75 (*t*, C-1), 37.09 (*s*, C-10), 34.25 (*t*, C-21), 33.40 (*c*, C-29), 32.72 (*t*, C-22), 31.22 (*t*, C-7), 31.14 (*s*, C-20), 28.27 (*c*, C-23), 27.33 (*t*, C-15), 26.14 (*c*, C-27), 25.70 (*t*, C-2), 23.77 (*c*, C-30), 23.70 (*t*, C-16), 22.12 (*t*, C-11), 18.53 (*t*, C-6), 16.89 (*c*, C-26), 15.79 (*c*, C-24), 15.71 (*c*, C-25); EIMS *m/z*: 442 [M+] (5), 279 (9), 256 (32), 213 (13), 203 (64), 167 (16), 149 (51), 129 (115), 91 (27), 69 (37), 50 (100). HR EIMS *m/z* 442.3830 [M$^+$] (Calculated for C$_{30}$H$_{50}$O$_2$, 442.3811).

4.2. Biological assays

4.2.1. Expression and purification of recombinant PTPases

The T-cell PTP (TC-PTP) was purchased from New England Bio-labs Inc.. Human PTP-1B, IF1 and IF2 isoenzymes of LMW-PTP were purified as fusion protein with GST by bacterial cell lines. Shortly, the complete sequence of PTP-1B, IF1, IF2 were cloned in the pGEX-2T bacterial expression vector downstream the GST sequence and those vectors were used to transform *Escherichia coli* to TB1 cell line. After, cells were lysate for recombinant fusion proteins purification using a single step affinity chromatography on glutathione-agarose. The solution with fusion protein was treated with thrombin for 3 h at 37 °C; next, the active phosphatases were purified from GST and thrombin by gel filtration on a Superdex G75 column. The purity was determined by SDS-PAGE.

4.2.2. Enzymatic inhibition

The inhibitory capacity of compounds were carried out at 37 °C using *p*-nitrophenylphosphate as substrate, dissolved in 1 mL 0.075 M of β,β-dimethylglutarate pH 7.0 buffer supplemented with 1 mM EDTA and 1 mM dithiothreitol. The reactions were started by adding aliquots of the enzyme and stopped with 4 ml of 1 M KOH at appropriate times. The quantification of produced *p*-nitrophenolate ion was measured by reading the absorbance at 400 nm ($e = 18,000$ M^{-1} cm^{-1}). The kinetic parameters K_m and V_{max} were determined by quantifying the initial rates of eight different substrate concentrations ranging from 0.5 to 40 mM. All data were analysed by Michaelis equation and a nonlinear fitting program (Fig-Sys). To verify if compounds **1**, **3**, **5**, **6**, and **11** were reversible inhibitors, appropriate aliquots of PTP1B were incubated in the presence of at least 25-fold molar excess of inhibitor for 1 h at 37 °C. Control experiments were performed adding DMSO instead of inhibitor. After this interval time, the enzyme solutions were diluted 400-fold and the residual enzyme activity was assayed.

4.2.3. Induction of NIDDM model

Groups of six male Wistar rats with 200–250 g of body weight were maintained at 25 ± 2 °C, 12 h light/dark cycle and 45–65% of humidity during experimental time. All animal procedures were developed in accordance with Mexican Federal Regulations for Animal Experimentation and care (SAGARPA, NOM-062-ZOO-1999, Mexico), and approved by the Institutional Animal Care and Use Committee (UNAM) based on US National Institute of Health publication #85-23, revised 1985. 16 h previous to diabetes induction all rats were fasted but had access to water ad libitum. Hyperglycaemia was induced by intraperitoneal administration of 110 mg/kg of nicotinamide 15 min before i.p. injection of 65 mg/kg of streptozotocin (Sigma–Aldrich Co. St. Louis, MO, USA) dissolved in citrate buffer pH 4.5. Diabetes was confirmed by raised plasma glucose over 200 mg/dL measured by a glucometer (Roche Accu-Check Performa, Mexico City, Mexico).

4.2.4. Antidiabetic assay

Fasted diabetic rats of experimental groups ($n = 6$) were administered *per os* a suspension of designed compound (50 mg/kg), metformin (reference drug, 120 mg/kg) or vehicle (Tween 80, 10%, 1 mL). Glucose concentration was determined from rat tail at 0, 1, 3, 5 and 7 h after administration with glucometer (Roche Accu-Check Performa, Mexico City, Mexico). The percentage of glycaemia was calculated by comparing a selected time glycaemia (G_x) with initial value (G_0) using the formula: %Variation of glycaemia = $[(G_x - G_0)/G_0] \times 100$. All values were expressed as mean $\pm$ S.E.M. Statistical significance was estimated by two-way ANOVA, $p < 0.05$ and $p < 0.01$ implies significance.

4.3. Docking

Both compounds were docked with the crystallographic structure of PTP-1B from Protein Data Bank (PDB code 1C83, resolution of 1.8 Å and cocrystallized with 6-(oxalyl-amino)-1*H*-indole-5-carboxilic acid). Docking studies were developed by selecting two sites previously described as important regions for PTP-1B inhibition. First of all, catalytic site or site A conformed by Asp181, Cys215 and Arg221, also Lys120, Ser216, Phe182, Gly220 are important residues for interaction inside this region. Further, an allosteric region known as site B composed by Arg24, Arg254, Gln262, Tyr46, Asp48, Val49, Ile219 and Met258 residues. Docking calculations were conducted with AutoDock 4.2, the auxiliary program AutoGrid generate the grid maps centred at $X = 48.136$, $Y = 7.931$ and $Z = 2.961$ and the grid dimensions were $60 \times 60 \times 60$ Å with points separated by 0.375 Å for including both sites. Before docking experiments, the protocol was validated by docking the co-crystalized ligand and obtaining a RMSD of 0.33 Å. Briefly, AutoDock performs an automated docking of the ligand with user-specified dihedral flexibility within a protein rigid binding site. The program performs several runs in each docking experiment, each run provides one predicted binding mode. All water molecules and 6-(oxalyl-amino)-1*H*-indole-5-carboxilic acid were removed from the crystallographic structure and all hydrogen atoms were added. For all ligands and protein, Gasteiger charges were assigned and nonpolar hydrogen atoms were merged, all torsions were allowed to rotate during docking. Lennard−Jones parameters were used for modelling H-bonds and Van der Waals interactions, the Lamarkian genetic algorithm was applied for the search using default parameters. The number of docking runs was 100, all solutions were clustered into groups with RMS lower than 1 Å after docking and the clusters were ranked by the lowest energy representative of each cluster. In order to describe the ligand-binding pocket interactions, the top ranked binding mode found by AutoDock in complex with the selected binding region of PTP-1B was subject to full energy minimization using MMFF94 force field. PyMOL 1.0 was used to generate the molecular surface of docking models.

Appendix A. Supplementary data

Supplementary data related to this article can be found at http://dx.doi.org/10.1016/j.ejmech.2014.09.036.

References

[1] T.O. Johnson, J. Ermolieff, M.R. Jirousek, Protein tyrosine phosphatase 1B inhibitors for diabetes, Nat. Rev. Drug. Discov. 1 (2002) 696−709.
[2] Y.B. Tang, D. Lu, Z. Chen, C. Hu, Y. Yang, J.Y. Tian, F. Ye, L. Wu, Z.Y. Zhang, Z. Xiao, Design, synthesis and insulin-sensitising effects of novel PTP1B inhibitors, Bioorg. Med. Chem. Lett. 23 (2013) 2313−2318.
[3] A. Alqahtani, K. Hamid, A. Kam, K.H. Wong, Z. Abdelhak, V. Ramzmovski-Naumovski, K. Chan, K.M. Li, P.W. Groundwater, G.Q. Li, The pentacyclic triterpenoids in herbal medicines and their pharmacological activities in diabetes and diabetic complications, Curr. Med. Chem. 20 (7) (2013) 908−931.
[4] Q.C. Liu, T.T. Guo, L. Zhang, Y. Yu, P. Wang, J.F. Yang, Y.X. Li, Synthesis and biological evaluation of oleanolic acid derivatives as PTP1B inhibitors, Eur. J. Med. Chem. 63 (2013) 511−522.
[5] D. Popov, Novel protein tyrosine phophatase 1B inhibitors: interaction requirements for improved intracellular efficacy in type 2 diabetes mellitus and obesity control, Biochem. Biophys. Res. Commun. 410 (3) (2011) 377−381.

[6] J.J. Ramírez-Espinosa, M.Y. Rios, S. López-Martínez, F. López-Vallejo, J.L. Medina-Franco, P. Paoli, G. Gamici, G. Navarrete-Vázquez, R. Ortiz-Andrade, S. Estrada-Soto, Antidiabetic activity of some pentacyclic acid triterpenoids, role of PTP-1B: *in vitro, in silico* and *in vivo* approaches, Eur. J. Med. Chem. 46 (6) (2011) 2243–2251.

[7] S. Thareja, S. Aggarwal, T.R. Bhardwaj, M. Kumar, Protein tyrosine phosphatase 1B inhibitors: a molecular level legitimate approach for the management of diabetes mellitus, Med. Res. Rev. 32 (3) (2012) 459–517.

[8] Y.A. Puius, Y. Zhao, M. Sullivan, D.S. Lawrence, S.C. Almo, Z.Y. Zhang, identification of a second aryl phosphate-binding site in protein-tyrosine phosphatase 1B: a paradigm for inhibitor design, Proc. Natl. Acad. Sci. 94 (1997) 13420–13425.

[9] H.S. Andersen, L.F. Iversen, C.B. Jeppesen, S. Brannen, K. Norris, H.B. Rasmussen, K.B. Moller, N.P. Moller, 2-(oxalylamino)-benzoic acid is a general, competitive inhibitor of protein-tyrosine phosphatases, J. Biol. Chem. 275 (2000) 7101–7108.

[10] S. Qian, H. Li, Y. Chen, W. Zhang, S. Yang, Y. Wu, Synthesis and biological evaluation of oleanolic acid derivatives as inhibitors of protein tyrosine phosphatase 1B, J. Nat. Prod. 29 (73) (2010) 1743–1750.

[11] S. López-Martínez, G. Navarrete-Vazquez, S. Estrada-Soto, I. León-Rivera, M.Y. Rios, Chemical constituents of the hemiparasitic plant *Phoradendron brachystachyum* DC Nutt, Nat. Prod. Res. 27 (2) (2013) 130–136.

[12] F. Hichri, H.B. Jannet, J. Cheriaa, S. Jegham, Z. Mighri, Antibacterial activities of a few prepared derivatives of oleanolic acid and of other natural triterpenic compounds, C. R. Chim. 6 (2003) 473–483.

[13] R. Weis, W. Seebacher, Complete assignment of ^{1}H and ^{13}C NMR spectra of new pentacyclic triterpene acid benzyl esters, Magn. Reson. Chem. 40 (2002) 455–457.

[14] K. Nam-Cheol, A.E. Desjardins, C.D. Wu, A.D. Kinghorn, Activity of triterpenoid glycosides from the root bark of *Mussaenda macrophylla* against two oral pathogens, J. Nat. Prod. 62 (1999) 1379–1384.

[15] X. Wen, H. Sun, J. Liu, K. Cheng, P. Zhang, L. Zhang, J. Hao, L. Zhang, P. Ni, S.E. Zographos, D.D. Leonidas, K.M. Alexacou, T. Gimisis, J.M. Hayes, N.G. Oikonomakos, Naturally occurring pentacyclic triterpenes as inhibitors of glycogen phosphorylase: synthesis, structure-activity relationships, and X-ray crystallographic studies, J. Med. Chem. 51 (2008) 3540–3554.

[16] V.U. Ahmad, A.U. Rahman, Hanbook of Natural Products Data, in: Pentacyclic Triterpenoids, vol. 1, Elsevier, Amsterdam, 1994, p. 67.